Persistent brainwave disruption and cognitive impairment induced by acute sarin surrogate sub-lethal dose exposure

Loïc Angrand, Samir Takillah, Isabelle Malissin, Asma Berriche, Chloe Cervera, Rosalie Bel, Quentin Gerard, Julie Knoertzer, Rachid Baati, Joseph P Kononchik, et al.

Version of Record: https://www.sciencedirect.com/science/article/pii/S0300483X21001104
Manuscript_4e9a8c27bf51edfe0fe9c404751f55dd

Persistent brainwave disruption and cognitive impairment induced by acute sarin surrogate sub-lethal dose exposure.

Loïc ANGRAND[1,2,3*]; Samir TAKILLAH[4,5*]; Isabelle MALISSIN[6]; Asma BERRICHE[1,7]; Chloe CERVERA[1]; Rosalie BEL[1]; Quentin GERARD[1,8]; Julie KNOERTZER[1]; Rachid BAATI[9]; Joseph P. KONONCHIK[1]; Bruno MEGARBANE[5]; Karine THIBAULT[1*]; Gregory DAL BO[1*]

1. Departement of Toxicology and Chemical Risks, French Armed Forces Biomedical Research Institute, Bretigny sur Orge, France.
2. EnvA, IMRB, Maisons-Alfort, France.
3. Université Paris-Est Créteil, INSERM, Team Relaix, Créteil, France
4. Departement of Neuroscience, Unit of Fatigue and vigilance, French Armed Forces Biomedical Research Institute, Bretigny sur Orge, France.
5. VIFASOM team (EA 7330), Paris Descartes University, Sorbonne Paris Cité, Hôtel Dieu, Paris, France.
6. Department of Medical and Toxicological Critical Care, Lariboisière Hospital, Federation of Toxicology APHP, Paris-Diderot University, INSERM UMRS-1144, Paris, France.
7. CEA, Fontenay aux roses, France.
8. Normandie University, UNICAEN, INSERM, GIP Cyceron, Institut Blood and Brain @Caen-Normandie (BB@C), UMR-S U1237, Physiopathology and Imaging of Neurological Disorders (PhIND), Caen, France.

9. ICPEES UMR CNRS 7515, Institut de Chimie des Procédés, pour l'Energie, l'Environnement, et la Santé, Strasbourg, France.

* Equal contribution

Corresponding Authors:

Gregory DAL BO

Institut de recherche biomédicale des armées

1 Place Général Valérie André, BP 73

91223 Brétigny sur Orge cedex

France

E-mail : greg.dal-bo@chemdef.fr

Karine THIBAULT

Institut de recherche biomédicale des armées

1 Place Général Valérie André, BP 73

91223 Brétigny sur Orge cedex

France

E-mail : karine.thibault@def.gouv.fr

Abstract:

Warfare neurotoxicants such as sarin, soman or VX, are organophosphorus compounds which irreversibly inhibit cholinesterase. High-dose exposure with nerve agents (NA) is known to produce seizure activity and related brain damage, while less is known about the effects of acute sub-lethal dose exposure. The aim of this study was to characterize behavioral, brain activity and neuroinflammatory modifications at different time points after exposure to 4-nitrophenyl isopropyl methylphosphonate (NIMP), a sarin surrogate. In order to decipher the impacts of sub-lethal exposure, we chose 4 different doses of NIMP each corresponding to a fraction of the median lethal dose (LD_{50}). First, we conducted a behavioral analysis of symptoms during the first hour following NIMP challenge and established a specific scoring scale for the intoxication severity. The intensity of intoxication signs was dose-dependent and proportional to the cholinesterase activity inhibition evaluated in mice brain. The lowest dose (0.3 LD_{50}) did not induce significant behavioral, electrocorticographic (ECoG) nor cholinesterase activity changes. Animals exposed to one of the other doses (0.5, 0.7 and 0.9 LD_{50}) exhibited substantial changes in behavior, significant cholinesterase activity inhibition, and a disruption of brainwave distribution that persisted in a dose-dependent manner. To evaluate long lasting changes, we conducted ECoG recording for 30 days on mice exposed to 0.5 or 0.9 LD_{50} of NIMP. Mice in both groups showed long-lasting impairment of theta rhythms, and a lack of restoration in hippocampal ChE activity after 1-month post-exposure. In addition, an increase in neuroinflammatory markers (IBA-1, TNF-α, NF-κB) and edema were transiently observed in mice hippocampus. Furthermore, a novel object recognition test showed an alteration of short-term memory

in both groups, 1-month post-NIMP intoxication. Our findings identified both transient and long-term ECoG alterations and some long term cognitive impairments following exposure to sub-lethal doses of NIMP. These may further impact morphopathological alterations in the brain.

Keywords: nerve agent, sarin surrogate, 4-nitrophenyl isopropyl methylphosphonate, sublethal exposure, brain waves, neuroinflammation.

List of abbreviations

AChE: acetylcholinesterase

AUC: area under the curve

CA1: cornu ammonis 1of hippocampus

ChE: cholinesterase

CNS: central nervous system

CTL: control mice

CWA: chemical warfare agent

DFP: diisopropyl fluorophosphate

ECoG: electrocorticographic

EEG: electroencephalographic

GFAP: glial fibrillary acidic protein

HF: hippocampal formation

HPS: Hemalun-Phloxin-Safran staining

IBA1: ionized calcium binding adaptor molecule 1

IL-1β: interleukin 1β

IL-6: interleukin 6

LD_{50}: median lethal dose

MIP-1α: macrophage inflammatory protein 1 α

NA: nerve agents

NF-κB: nuclear Factor kappa-light-chain-enhancer of activated B cells

NIMP: 4-nitrophenyl isopropyl methylphosphonate

NORT: novel object recognition test

OF: open-field box

OP: organophosphorus

PFA: paraformaldehyde

SEM: standard errors of the mean

TNF-α: tumour necrosis factor alpha

VEGF: vascular endothelial growth factor

Introduction:

The 2010s have been marked by the resurgence of organophosphorus (OP) chemical warfare agent (CWA) use in various scenarios. Sarin was reported in numerous attacks between 2013 and 2017, causing deaths and casualties in both civilian and military populations (Amend et al., 2020; John et al., 2017). Two others nerve agents (NA), VX and Novichok were used in targeted attacks, leading to the death of Kim Jong Nam in 2017 (Amend et al., 2020) and the direct poisoning of Sergei and Yulia Skripal in 2018, and Alexei Navalny in 2020 (Amend et al., 2020; Chai et al., 2018; Greathouse et al., 2020). Despite the progress to eliminate chemical weapon stockpiles, the ongoing tangible threat of OP derivative compounds has persisted. In addition, the important use of OP containing pesticides still accounts for more than 1 million poisonings worldwide (Abou-Donia et al., 2016; Eddleston, 2019).

OP compounds are irreversible cholinesterase (ChE) inhibitors that lead to a toxic accumulation of acetylcholine in synapses and neuromuscular junctions. After exposure to some OPs, a large range of symptoms occur in victims including fasciculation, hypersecretion, and muscle twitching, which can culminate in respiratory distress, epileptic seizure, and death (Abou-Donia et al., 2016). When exposed to high doses of OP, death results from respiratory failure due to muscles paralysis and bronchoconstriction, though it can be avoided if emergency therapy (atropine sulfate and an oxime, a strong nucleophile able to reactivate OP-inhibited acetylcholinesterase (AChE)) is quickly administered. However, the OP effects in the central nervous system (CNS) may not be stopped quickly enough by this intervention if it is delayed, and their neurotoxicity may lead to epileptic seizures and subsequent brain damage (Dail et al.,

2019; de Araujo Furtado et al., 2010). While the neurotoxic effects of lethal or supra-lethal NA doses have been extensively studied (Grauer et al., 2008; Schultz et al., 2014; Testylier et al., 2007), the cerebral impact of acute sub-lethal doses of NA have been poorly investigated. Also, due to the heterogeneity of intoxication protocols used, controversy persists on the neurophysiological changes and cellular alterations of those doses. Though single sub-lethal doses of soman failed to induce marked histopathological damage in exposed animals (Baille et al., 2001), anxious behavior and cognitive deficits could be transiently observed following NA exposure (Baille et al., 2001; Crouzier et al., 2004; Genovese et al., 2009; Kassa et al., 2004; Pearce et al., 1999), which contrasts with the report that no memory impairment was observed below a threshold of 15% neuronal loss (Filliat et al., 1999). It is also interesting that electroencephalographic (EEG) or electrocorticographic (ECoG) recordings seem to be only transiently disturbed if 50% of brain cholinesterases are inhibited (Crouzier et al., 2004; Pearce et al., 1999). Neural oscillatory patterns were altered in the first hours following soman exposure in mice, with an increase in delta power coupled to a decrease in theta (Crouzier et al., 2004). At later stages, these changes in power are compensated within the first 24h after exposure, and only sleep stages are still altered up to 1 week (Crouzier et al., 2004). Nevertheless, sub-lethal sarin doses induced long-term EEG/ECoG abnormalities in marmoset (van Helden et al., 2004) consistent with the reports on Tokyo's victims (Yanagisawa et al., 2006). Furthermore, sub-chronic VX exposure at $0.3LD_{50}$ was determined to be the threshold to elicit fluctuations in theta and alpha waves 4 weeks after the initial exposure in rats (Bloch-Shilderman et al., 2018). Therefore, more extensive characterization of the acute and long-term changes in EEG/ECoG recordings of sub-lethal doses of NA is needed.

One of the major limitations studying NA neurotoxicity is based on the restrictions for obtaining CWA. Considering the re-emergence of NA threat, the use of surrogates offers an alternative to extend investigating methods to unauthorized laboratories. A promising sarin surrogate was obtained by the synthesis of 4-nitrophenyl isopropyl methylphosphonate (NIMP) (Meek et al., 2012; Ohta et al., 2006). This non-volatile compound is safer to use, efficiently inhibits cholinesterases, and is more potent and more stable in solution than diisopropyl fluorophosphates (DFP) (Chambers and Meek, 2020; Chambers et al., 2016; Meek et al., 2012). *In vivo* challenges with sub-lethal and/or lethal doses of NIMP elicit signs of OP intoxication, seizure-like behavior, and significant neuronal damage in rats (Chambers et al., 2016; Dail et al., 2019). Furthermore, NIMP exposure notably results in cellular injury and astrocytic activation in the piriform cortex and hippocampus, which are some of the most affected cerebral regions by NA (Pringle et al., 2018). Nonetheless, a deeper characterization of NIMP exposure will be needed to confirm its potency to mimic CWA.

The aim of this study was to test NIMP exposure in mice, report symptoms following a single exposure of different sub-lethal OP doses, and characterize a typical EEG/ECoG 'fingerprints' at key-points after intoxication. We thus evaluated the behavioral effects of four different doses (0.3, 0.5, 0.7 and 0.9 LD_{50}) of NIMP during the first hour following mice exposure. Cerebral cholinesterase inhibition, neuroinflammation and signalling changes were evaluated at different time points up to 30 days post-exposure. In parallel, ECoG were recorded for 24 hours for each dose to differentiate the acute signs of intoxication and the brainwave changes at early stages. Afterwards, telemetric ECoG

recording was performed to follow the perturbations over 1 month. At 1 month after NIMP exposure, potential cognitive impairments were evaluated.

Material and methods

Animals

All experimental procedures were approved by the French “Service de Santé des Armées” animal ethics committee according to the applicable French legislations (Directive 2010/63/UE, décret n°2013-118). Adult male Swiss mice (Janvier Labs, France) aged from 6 to 8 weeks were housed, four per cage, with a 12h/12h light/dark cycle temperature-controlled room (22 ± 2°C), food, and water available *ad libitum*. After 7 days of acclimation period, the animals were brought to their dedicated experiment. All animals were 9-week old at the OP challenge.

NIMP exposure

4-nitrophenyl isopropyl methylphosphonate (NIMP, Fig sup. 1) used as a sarin surrogate was synthesized by Rachid Baati (Université Strasbourg, ICPEES UMR CNRS 7515, France) as previously described (Meek et al., 2012), with almost identical purity, determined by ^{1}H NMR (mass %: 92%). The day of the experiment, mice received a single subcutaneous injection (10ml/kg) of NIMP (LD_{50} = 0.63mg/kg), freshly diluted in 0.9% NaCl at one of 4 sub-lethal doses (0.3, 0.5, 0.7, or 0.9 LD_{50}). Control mice (CTL) received a similar vehicle injection without NIMP. For the preceding hour and the days following NIMP exposure the weight of the mice was monitored and behavioral assessment was conducted to evaluate their recovery (Fig. sup. 2).

Behavioral observation

Intoxication severity scale:

Several typical signs of cholinergic toxicity such as hypersecretion, tremor, loss of posture, etc., have been extensively described (Bloch-Shilderman et al., 2018;

Senanayake et al., 1993; Shih and Romano, 1988); with a modified Racine's scale used to evaluate epileptic behavior (de Araujo Furtado et al., 2010; Enderlin et al., 2020; Phelan et al., 2015). Considering that the lowest doses used in our study would elicit more subtle signs, all mice were observed and videotaped during the first hour post-intoxication. All behavioral changes observed in NIMP exposed mice, compared to control animals, were noted with their onset, and considered as observable signs of intoxication. Finally, 13 signs of intoxication were selected, grading animals from normal (=0) to death (=12). For this study, 336 mice were evaluated to include 83 control animals.

Novel object recognition (NOR) test:

Mice were placed in an empty open-field (OF) box for a 10min habituation period. Before and 1 month after NIMP exposure, mice of 3 groups (CTL n=15; 0.5 LD_{50} n=15; 0.9 LD_{50} n=17) were placed in the same OF box with 2 identical objects, allowed to explore for 5 min, then returned to their home cage. After 1 hour, the mice were placed in the OF containing 1 familiar object and a novel object and allowed to explore for 5 min. The objects were placed at the same locations as the first session. All NOR sessions were videotaped and the exploration time was analyzed using EthoVision XT software (Noldus, NL).

Surgery

Two different ECoG procedures were used in this study that followed the same surgery protocol. Seven-week old mice were anesthetized in an induction box using isoflurane (5% in oxygen at L/m). They were injected with buprenorphine (Bupredine®, 0.1 mg/kg, i.p.), and prepared for surgery. Their head was shaved and lidocaine (Lurocaine®,

5mg/kg, s.c.) was applied on their scalp before being placed in a stereotaxic apparatus and maintained with inhalation of a mixture of isoflurane (2%) and oxygen (100%).

Wired ECoG recordings were used for 24-hour recordings (70 mice divided in five groups). After skin incision, 3 holes were drilled with the recording holes positioned over the left and right parietal cortices (AP -2mm; L ±1.75mm) and the third one over the cerebellum (AP -6.5mm) for reference. In each hole a stainless steel screw was inserted and bipolar cortical electrodes with ground (MS333/2-BIU/SPC, Plastics One, U.S.A.) were connected to the screw. Composite resin was wrapped around skull screws to secure the device.

For ***Telemetric ECoG*** (22 mice divided in 2 groups), only 2 holes were drilled over the parietal cortices (same coordinates). The screws were connected to flexible leads of a biopotential transmitter (ETA-F10, DSI, USA) subcutaneously implanted in the mouse's flank according to the manufacturer's protocol. The screws were wrapped with adhesive resin cement and covered with sterilized silicone paste. Then, the scalp was sewed.

All the mice were permitted to recover until regaining pre-surgery body weight and returned to their home cage for a 2-week complete recovery period before being recorded and exposed to NIMP.

ECoG recording and power spectra analysis

For wired ECoG recordings, 4 animals per experimental day were connected via a cable to a data acquisition system for a 24h recording period. Cerebral electrical activity was recorded using the customized Brain Quick EEG system (MicroMed, Treviso, Italy). Baseline activity was recorded for 1 hour before NIMP exposure.

For telemetric recording, 8 animals were recorded simultaneously using DataQuest acquisition software (DSI, USA). In addition to ECoG, subcutaneous temperature,

animal activity, and transmitter power were also recorded. Baseline cerebral activity was recorded for 4 hours the day before the intoxication challenge and 1 hour before intoxication. Mice were recorded continuously for the first 24 hours and then for 2 hours session per day the rest of the first week. Following the first week, two 2-hour recording sessions were conducted per week. Data were analyzed using Matlab (Matworks®, USA) built-in functions and chronux toolbox (Bokil et al., 2010). ECoGs were (i) acquired at 512Hz and offline band-pass filtered at 0.1-128Hz with zero-phase shift filter function (zero-phase digital filtering *filtfilt* function), and (ii) detrended using a local linear regression (*locdetrend* function: window-size 1s, overlap 0.5s) to remove slow drifts, and (iii) notch-filtered (*iirnotch* function) with notch located at 50Hz to remove possible power line noise. Power spectrum of ECoG data was calculated using the multi-taper time-frequency spectrum method (*mtspecgramc* function) with time-bandwidth product of 30 and 59 Slepian sequences of orthogonal data tapers (windows-size 30s, 10s overlap).

The ECoG power spectrum was divided in the following bands: delta (0.5-4 Hz), low theta (4-8 Hz), high theta (8-12 Hz), low beta (12-16 Hz) and high beta (16-25 Hz) using Neuroscore software (DSI, St-Paul, MN, USA). Mean power was calculated for each band for 30s epochs. For each animal, data from telemetric recording are normalized to the pre-intoxication baseline recording values. Spontaneous electrical reactivity was defined by the modifications in the background activity (acceleration or slowing) in relation to the spontaneous fluctuations in arousal level. Encephalopathy was stratified using Markand's classification (Markand, 1984).

Cholinesterase activity and multiplex biomarker assays

At different time points (6 and 24 hours, 3 and 7 days, and 1-month) after NIMP exposure, animals were deeply anaesthetized with pentobarbital, a sample of blood was

collected, and the mice were transcardially perfused with cold 15 ml of 0.9% NaCl. Brains were quickly removed and dropped in cold saline before being sliced in 2mm thick coronal sections. Hippocampus were micro-dissected, collected in Eppendorf tubes and frozen on dry ice. The hippocampal samples were homogenized in 50 mM phosphate buffer (pH 7.4)/0.5% Tween using a bead mill homogenizer (OMNI International) with 1.4 mm ceramic beads and centrifuged at 10,000 X g (4 °C) for 10 min. The resulting supernatants were stored at −80°C. Total protein concentrations were determined using a DC Protein Assay (Bio-Rad).

Cholinesterase inhibition assay: AChE activity was determined using the Ellman method by adding 5 µl of hippocampus sample to 0.22 mM 5,5′-dithiobis-2-nitrobenzoic acid (DTNB, Sigma Aldrich) plus 0.1 mM ethopropazine hydrochloride (Sigma Aldrich) to inhibit butyrylcholinesterase**.** After a 15min baseline measurement, 1 mM acetylthiocholine (Sigma Aldrich) was added and the reaction between thiocholine and DTNB was monitored for 30 min at 412 nm and 25 °C by a microplate reader. All samples were assayed in duplicate. The ChE activities of the hippocampal samples were normalized with total protein concentration for each sample. The final results were expressed as percentages of average control activity.

Milliplex multiplex assays: Cerebral concentrations of IL-1β, IL-6, MIP-1α, TNF-α, and VEGF were obtained by using the Milliplex MCYTMAG-70K-PX32. NF-κB hippocampal levels were analyzed using Milliplex 48-681MAG (EMD Millipore, USA) and the Bio-Plex MAGPIX multiplex reader (Bio-Rad, USA).

Histology

At different time points (24 hours, 7 days, and 1-month) post NIMP exposure, mice were deeply anaesthetized with pentobarbital, and transcardially perfused with cold 10 ml of 0.9% NaCl, followed by 30 ml of 4% paraformaldehyde (PFA) in phosphate buffer. Brains were quickly removed and immerged in cold 4% PFA for overnight post-fixation. The brains were cryoprotected 24-48h in cold 20% sucrose and then frozen in -40°C isopentane. All brains were sliced in 14 µm coronal sections using a cryostat and the slices were sequentially mounted on Superfrost+ slides (VWR, USA). For 1 slide per animal, common Hemalun-Phloxin-Safran (HPS) staining was conducted to evaluate neuronal damage and neuroanatomic changes. HPS labeled slices were imaged with a digital microscope system (K1300, Hirox, CN). For each animal, 3 slices containing septal hippocampus were analyzed. Immunofluorescent labelling with mouse anti-GFAP (1/1000, MAB360, Millipore) and rabbit anti-IBA1 (1/1000, Wako, USA) were detected by anti-mouse 488 and anti-rabbit 555 respectively (both at 1/500, Invitrogen, USA) to analyze astrocytic and microglial activity. The fluorescently labelled CA1 part of the septal hippocampus was imaged using an automated Leica DM6000 B research microscope (Leica Microsystems, DE), analyzing 3 slices per animal. All acquisitions were performed with the same acquisition setup. Stereotaxic consistency between animals was provided by using the reference mouse brain atlas (Gf and Franklin, 2003). Analysis was performed using the ImageJ software. To quantify Iba1 or GFAP staining, we performed an area fraction analysis. Briefly, a threshold is set, and pixels in the image whose value lie above the threshold are converted to white, while pixels with values below the threshold are converted to black. The threshold was determined to obtain clear area representing IBA1 or GFAP labelling in control animals. The same

threshold was applied on each image of all animal groups. This analysis measured the area of labelling in regions of interest.

Statistics

Data were expressed as means ± standard error of the mean (SEM) and analyzed using PRISM 7 software (GraphPad, U.S.A.). Statistical tests and sample sizes are indicated in figure legends and figures respectively. Results are presented as mean ± SEM. Significance between groups are denoted by * $p < 0.05$, ** $p < 0.01$, *** $p < 0.001$, or **** $p < 0.0001$.

Results

Intoxication severity scale:

To discriminate between the most common intoxication signs induced by sub-lethal doses of NIMP, we conducted preliminary experiments over the first hour following NIMP exposure. We identified 22 signs that elicited significant behavioral changes compared to the CTL mice. To avoid experimental biases, 6 “treatment-blinded” experimenters noted the occurrence and the onset of signs. Data compilation for the 4 studied sub-lethal doses of NIMP allowed the selection of the 12 most prevalent behavioral changes, and established a severity scale based on the appearance percentage and time of each sign (Fig. 1B-E). Animals that did not show any behavioral perturbation were scored 0. Selected signs were classed and mice were attributed the highest number reached after NIMP exposure (Fig. 1B). The lowest dose (0.3 LD_{50}) caused fasciculation restricted to the injection site in less than half of the animals, and the mice recovered quickly. At this dose no other intoxication sign was observed and the mice were scored 1 based on our severity scale. Almost all mice exposed to 0.5 LD_{50} of NIMP displayed fasciculation, stereotypies (chewing) and first signs of respiration difficulty (yawning). One fifth of 0.5 LD_{50}-exposed mice showed transient muscle weakness and excessive thoracic kyphosis with a few animals at this dose also presenting light head bobbing and rare muscular spasms. With the following dose (0.7 LD_{50}), the majority of animals quickly presented the first 6 signs as well as involuntary twitching that persisted over the 1-hour observation period. When exposed to this dose, a few animals also showed peripheral epileptiform behaviors that were differentiated into a short-time period (head or upper body part convulsion <5s, with rest periods) and episodic total body myoclonus (>10s, with calm periods) lasting for few minutes (< 30

min). Note that we used “convulsion” to describe the intense uncontrolled tremors when electrical seizure cannot be ensured. One mouse exposed to 0.7 LD_{50} of NIMP showed generalized convulsions that lasted more than 30 min. Finally, the highest tested dose (0.9 LD_{50}) provoked all the previously cited symptoms in a short time (< 20 min) and was also characterized by the incidence of long-lasting convulsions in 78% of animals. In half of 0.9 LD_{50} exposed mice, bulging eyes were observed, but only in animals with long lasting convulsions that preceded generalized convulsions. Only 5 animals exposed to the highest dose died, and all of them presented the 11 first symptoms.

NIMP exposed animals used for ECoG recording were also evaluated on the same scale, and for the same intoxication doses no significant difference was observed in the score severity between animals with and without surgery (Fig. 2B, 3B).

Cholinesterase activity:

Several brain areas including the hippocampus, thalamus, amygdala, and piriform cortex are known to be particularly sensitive to NA exposure. We chose to focus on HF due to its involvement in learning and memory processes as well as brain rhythm generation (Amilhon et al., 2020; França et al., 2014; Shi et al., 2021). Measurement of cerebral ChE activity following NIMP exposure was conducted at different time points after exposure on intact animals (without surgery). The lowest dose (0.3 LD_{50}) did not show significant difference in ChE activity compared to CTL mice (Fig. 2C). Otherwise, the other sub-lethal doses (0.5; 0.7; 0.9 LD_{50}) of NIMP induced robust hippocampal AChE inhibition at 6 and 24 hours after exposure in a dose-dependent manner (ranging from 75 to 90% respectively). These results seemed to be in agreement with the mild signs observed in 0.3 LD_{50} mice, as opposed to the other doses, which elicited clear intoxication symptoms in NIMP exposed animals. Similar inhibition patterns were

observed in blood samples regarding the different doses of NIMP evaluated (Fig. sup. 3). Measurement of hippocampal AChE activity in the long-term showed a persistent, significant inhibition on animals exposed to 0.5 or 0.9 LD_{50} of NIMP at up to 1 week, while recovery was still incomplete at 1-month post exposure (Fig. 3C).

Cortical activity modifications:

Short-term ECoG evaluation was conducted over 24 hours. Baseline cortical activity was recorded for 1-hour prior to NIMP challenge to ensure that EEGs were consistent across the 5 different groups studied (Fig. 2D). After NIMP exposure, or vehicle for CTL, cortical activity was recorded for 23 hours. Of the 77 animals recorded, only 57 presented suitable and complete recordings and were kept for brainwave analysis. Mice exposed to 0.3 LD_{50} did not present any change in cortical frequencies ranges in their power spectrum when compared to the CTL and their own baseline (Fig. 2E,F). In contrast, power spectrum for the complete period (24 h) of ECoG recordings showed a significant decrease of relative power in animals exposed to 0.5 or 0.9 LD_{50} of NIMP (Fig. 2E). In addition, spectrogram representation for the 3 doses showed a switch of theta rhythm dominance for delta rhythm, which lasted in a dose-dependent manner (Fig. 2F). The fall in all brainwave power spectrum was observed at different time periods in animals exposed to 0.5, 0.7 and 0.9 LD_{50} of NIMP, with significant decrease in high theta (8-12 Hz), low beta (12-16 Hz), and high beta (16-24 Hz) without recovery at 24h (Fig. 2G). In addition, brainwave distribution analysis showed an increase of delta rhythm (0.5-4 Hz) during the first 6 hours following 0.7 and 0.9 LD_{50} exposure. This correlated to a decrease in high theta rhythm (Fig. 2H). Interestingly, no electrical seizure was observed in any NIMP exposed animals during the 24-hour recording, even if they presented long-lasting convulsions.

Cortical activity modifications were then evaluated for up to 1-month on mice exposed to 0.5 or 0.9 LD_{50}. In this experiment, animals were their own control, so baseline activity was recorded during 2 periods, 24 hours and 1-hour before NIMP intoxication. A closed, blinded investigation of spontaneous cerebral activity was conducted by a neurologist. Four mice of each group were analyzed, and 2 out of the four mice treated with NIMP at 0.5 LD_{50} exhibited encephalopathy that peaked at 11 and 12 min after injection. Encephalopathy was moderate in two mice (maximum grades of 1 and 2), lasting 100 min and 24 h, respectively. The other two mice presented no changes in their ECoG cerebral activity. All four mice treated with NIMP at 0.9 LD_{50} exhibited more severe encephalopathy (maximum grade of 3 in three mice and 4 in one mouse), that occurred 6 (in 2 mice), 7, and 8 min after the injection (Fig. 3C). Again, no electrical seizures were observed at any selected time point over the month following exposure. However, sporadic “spike and wave”-like bursts were observed in 5 mice exposed to 0.5 LD_{50} and 8 mice exposed to 0.9 LD_{50}, which persisted over 30 days (Fig. 3D). Similar to wired animals, delta brainwave (0.5-4 Hz) distribution was significantly increased during the first 24 hours in the 0.9 LD_{50} exposed animals, but returned to normal 48 hours after exposure (Fig. 3E). In contrast, low theta (4-8 Hz) and high theta (8-12 Hz) brainwaves were persistently altered over the month in animals exposed to 0.9 LD_{50} (Fig. 3F, G). Once again, 0.5 LD_{50} exposure elicited mitigated brainwave perturbations, however a significant increase in low theta rhythm was still observable 30 days post-intoxication (Fig. 3F). No persistent modifications were observed in beta rhythms in any animal.

Histological modifications:

Morphological evaluation was conducted at 2 different time points after NIMP exposure. Seven days post-intoxication, a significant swelling was observed in hippocampal formation (HF) for both NIMP doses tested (Fig. 4B). The ratio of HF over total hemisphere areas was increased by 21% (±0.03) and 20% (±0.04) on 0.5 and 0.9 LD_{50} exposed animals, respectively, when compared to the CTL (Fig. 4C). However, this morphological difference was no longer evident 30 days post-NIMP exposure, as HF over the total hemisphere area ratio was equivalent to the CTL. In addition, microscopic analysis did not reveal any histopathologic difference between NIMP-exposed mice and the CTL.

Extensive examination of astrocytic reactivity in the hippocampus showed a slight, but non-significant, increase (44% ±25 and 42% ±9) of GFAP labelling in 0.5 and 0.9 LD_{50} NIMP exposed mice, respectively (Fig. 4D-G). This trend was not apparent 30 days post-NIMP exposure. Furthermore, 7 days post-intoxication, NF-κB expression was significantly increased in 0.5 LD_{50}-exposed animals (+ 104% NIMP ±40), and slightly increased in 0.9 LD_{50}-exposed animals (+ 45% NIMP ±21) (Fig. 4H). Again, these differences in NF-κB expression were not observed 30 days post-intoxication.

Induced neuroinflammation:

Cerebral cytokine levels were evaluated using Luminex technology (Moncunill et al., 2014). As suspected, sub-lethal doses of NIMP did not induce robust inflammation in mice hippocampus. Surprisingly, an early and transient increase in TNF-α and VEGF expressions was observed only in 0.5 LD_{50} mice 24h after NIMP exposure (Fig. 5B). Nevertheless, even if no significant cytokine level increase was present 7 days post-intoxication, the macrophage inflammatory protein 1-α (MIP-1-α or CCL3) expression was slightly increased in both groups (+48% ±37 for 0.5 LD_{50}; +116% ±43 for 0. 9LD_{50}

mice; Fig. 6B). In addition, microglia reactivation was significantly increased in 0.9 LD_{50} mice hippocampus at 24 hours, and persisted for up to 30 days post-intoxication (Fig. 6C-E). Microglia were moderately activated by the lower dose of NIMP, as a slight and transient increase was observed at 24 hours and 7 days post-intoxication in the 0.5 LD_{50} group (Fig. 6C).

Short-term memory impairment:

Considering that neuroinflammatory responses could alter cognitive functions, memory, and hippocampal synaptic activity (Barrientos et al., 2015; Jin et al., 2016; Marciniak et al., 2015), the mice of each group were subjected to recognition memory tests. Two sessions of object recognition tests were conducted before and 1 month after NIMP challenge (Fig. 6F). This test relies on a rodent's natural propensity to explore novelty and showed that all mice increased exploration (72.4% ± 3.9 for CTL; 75.4% ± 3.5 for 0.5 LD_{50}; 72.4% ± 3.9 for 0.9 LD_{50}) of the novel object during the baseline session before intoxication (Fig. 6G). One month after NIMP exposure, the exploration performance for the novel object significantly decreased in NIMP intoxicated animals (58.2% ± 2.3 for 0.5 LD_{50}; 54.7% ± 2.3 for 0.9 LD_{50}), while CTL mice kept their interest for the novel object (69.1% ± 3.6 for CTL) (Fig. 6G). No velocity modification was observed in any groups.

Discussion

Despite extensive efforts to ban the toxins, sarin and other CWA are still a major concern as evident by their use in the Syrian conflict and in targeted assassination attempts. In addition, follow-ups on victims exposed to sarin (Sugiyama et al., 2020) and to sarin combined with sulphur mustard (Talabani et al., 2018) have reported the prevalence of long-term neurological complications; suggesting the need to extend experimental research in order to identify biomarkers for novel targets and develop more effective antidotes to treat OP NA exposures. Considering that CWA restrictions limit the opportunity to investigate their effects, one of our goals was to confirm the reliability of a sarin surrogate (NIMP) in mice, and to develop a suitable animal model for studying long-term sub-lethal OP exposure effects. So far, research using NIMP exposure has been limited to rats. Developing a murine model will offer a good alternative and expand the breath of projects that use transgenic mice (Marrero-Rosado et al., 2020).

Initial *in vivo* research demonstrated that rats subjected to high sub-lethal or lethal doses of NIMP reproduced some typical features of NA intoxication, such as facial stereotypes, head and body tremors, fasciculations, myoclonic convulsions, seizure-like behaviors, and respiratory distress (Chambers et al., 2013; Chambers and Meek, 2020; Meek et al., 2012). Furthermore, NIMP challenges at high sub-lethal or lethal doses were able to respectively induce an astrocytic reactivation and a neurodegeneration in rats' piriform cortex and hippocampus; 2 cerebral regions that are particularly sensitive to OP intoxication (Dail et al., 2019; Pringle et al., 2018). The authors concluded that NIMP fits the requirements of a sarin surrogate in both *in vitro* and *in vivo* studies (Chambers and Meek, 2020).

As an initial step, we established a scoring scale to characterize the intoxication severity by challenging mice with 4 sub-lethal doses of NIMP. We determined that 0.5 LD_{50} is the threshold dose for NIMP to elicit significant behavioral changes, including facial stereotypes and yawning in the majority of exposed animals, and muscular weakness and thoracic kyphosis in 25% of them. This scale allows objective discrimination of the observed toxic symptomatology. Increasing the dose of NIMP results in more severe signs of intoxication (e.g. tremors, convulsions, eye bulb outgrowth). These symptoms were present in a time-dependent manner and in an increasing number of mice as the dose increased. Nevertheless, the threshold determined with our scale contrasted with some studies using sub-lethal doses of sarin in which no toxic signs were observed below 0.4 and 0.5 LD_{50} (Hulet et al., 2002; Oswal et al., 2013; Scremin et al., 2003). Taking into account species differences in NA intoxication sensitivity, types of NA, and intoxication routes, the dose-response symptomatology established in our study needs to be compared to a sub-cutaneous sarin challenge in mice directly, to confirm NIMP as a valuable sarin analog. However, the intoxication behavior severity score, as determined with our scale, is consistent with the percentage of hippocampal AChE activity inhibition observed at 6 and 24h post NIMP challenge. The most affected animals presented the highest levels of inhibition at both time points. Only the mice exposed to 0.3 LD_{50} did not show significant cerebral nor blood cholinesterase inhibition compared to control levels. In addition, no intoxication signs were observed in the majority of 0.3 LD_{50}-exposed mice, and less than half of the mice exposed to this dose only showed fasciculation restricted to the injection site. Furthermore, in ECoG recorded animals challenged with 0.3 LD_{50} of NIMP, no significant modification in brainwave power or distribution was observed; supporting the

sub-clinic toxicity at this dose. The three other doses induced significant cerebral AChE activity inhibition, more than 65%, with a culminating 94% inhibition 6 hours after 0.9 LD_{50} of NIMP exposure. Despite this massive inhibition of AChE activity, no electrical seizure activity was induced by any dose of NIMP, supporting that seizure initiation cannot be explained just by the AChE inhibition levels (González et al., 2020; Tonduli et al., 2001). Shortly after NIMP challenge with doses > 0.5 LD_{50}, all frequency ranges of the power spectrum declined. Remarkably, a transient enhancement of delta distribution was observed shortly after NIMP exposure, combined with a compensatory decrease in high theta activity, which lasted several hours and in a dose-dependent manner.

Increase in delta power distribution has been well characterized in different NA-exposed animal models, is observed prior to the start of seizure activity, and lasts several hours after the seizure onset (Carpentier et al., 2001; Crouzier et al., 2004; Lumley et al., 2019). In our study, the delta power distribution was significantly increased shortly after the challenge in mice exposed to the two highest doses of NIMP (0.7 and 0.9 LD_{50}), but normalized 6 hours post-intoxication. However, telemetric recordings showed a more sustained increase in delta power distribution for animals exposed to 0.9 LD_{50} that normalized 48 hours after exposure. The increase in delta power has been linked to the progression of neuropathology after soman induced seizures (Carpentier et al., 2001). Our results emphasize that even a long perturbation (> 5 h) of delta range is not sufficient alone to predict brain histopathology, as no significant neurodegeneration was observed in high sub-lethal doses at any point studied. These results are in line with previous reports on mice exposed to low or mild doses of soman (Baille et al., 2001; Crouzier et al., 2004). Consequently, the cholinergic toxicity induced by exposure to sub-lethal doses of NIMP did not result in neuronal damage, which emphasizes that seizure

activity is required to elicit significant neurodegeneration (González et al., 2020). Therefore, in the case of high sub-lethal exposure, the prevalent distribution of delta rhythms leads to grade 4 EEG abnormalities, which correspond to the unconscious state of animals (Guidera et al., 2017).

Nevertheless, ECoG recordings showed long-lasting disruption in low and high theta rhythms following NIMP challenge, including the 0.5 LD_{50} group. Theta brainwave modification was already reported in mice exposed to a low-dose of soman (Crouzier et al., 2004). During the 6 hours post-intoxication, a decrease in theta activity (6-9Hz) is observed, followed by an increase over the 2 next days (Crouzier et al., 2004). In this study we have divided the theta rhythm into a low (4-8 Hz) and a high (8-12 Hz) ranges, which, according to us, is a better brainwave representation (Buzsáki and Draguhn, 2004; Buzsaki et al., 2013). This division allowed us to interpret the high theta frequency as the alpha bandwidth found in higher mammal species (Buzsaki et al., 2013). In both 0.5 and 0.9 LD_{50} groups 1-month after NIMP exposure, we observed a significant increase in the low theta band distribution, associated with a compensatory decrease in the high theta rhythm. Similar results were obtained on corresponding bandwidths in rats after exposure to chlorpyrifos, an OP pesticide (Timofeeva and Gordon, 2002). Theta rhythm is commonly associated with the HF as it predominates in this area, and it is particularly modulated by cholinergic neurons from the medial septum (Ma et al., 2020). Considering that in the hippocampus we observed a long lasting AChE activity inhibition after NIMP exposure, it seems consistent that low-theta oscillations are still disrupted one month post-intoxication. Once again, our results underline the similarity between NIMP and sarin, as NIMP is showing the increase in delta and theta frequencies and the

decrease in alpha rhythm that were reported on industrial workers accidently exposed to undefined doses of sarin (Duffy et al., 1979).

Brainwave power modification could be predictive of cerebral complication, such as an increase of theta rhythm prior to electrical seizure onset (Karunakaran et al., 2016). Although, mice exposed to sub-lethal doses of NIMP did not elicit electrical seizure, the changes in their brainwave activity could be explained by the morphological modifications, i.e., hippocampal swelling, observed 1-week post-exposure. Both delta and theta rhythm abnormalities have been reported in cases of vasogenic edema (Fernández-Bouzas et al., 1999; Fernández-Bouzas et al., 2001). Increase in water diffusion in hippocampus has been reported in several magnetic resonance imaging studies, in mice as soon as 3 hours after intoxication with convulsive doses of soman (Testylier et al., 2007). It is still seen increasing 72 hours in rats exposed to seizing dose of DFP (Hobson et al., 2018), and is suggested to correlate to neurodegeneration (Lee et al., 2020). In our study, no neurodegeneration was found and the hippocampal edema was observed in the non-convulsive group (mice exposed to 0.5 LD_{50} of NIMP). A seizing state could disrupt the blood brain barrier and cause edema (Löscher and Friedman, 2020); however the sub-lethal doses used in our study were not sufficient to induce seizure in mice. So the hippocampal edema observed 7 days post-intoxication could be explained by an increase of astrocyte swelling induced by NF-κB activation as described in astrocyte culture (Jayakumar et al., 2014). A transient increase of NF-κB was associated with the increase of astrocyte reactivity in 0.5 LD_{50} group, 7 days post-intoxication. NF-κB could be rapidly activated in response to cellular aggression and homeostatic changes induced by an increase in pro-inflammatory cytokines (IL-1β and TNF-α), glutamate, and reactive oxygen species (Meffert et al., 2003). Also, sarin

surrogates could activate early genes like mitogen activated protein kinase, c-*jun* N-terminal kinase, and c-fos that modulate the astrocytic response (Damodaran et al., 2002; Damodaran et al., 2000; Niijima et al., 2000). Furthermore, a single exposure to 0.5 LD_{50} of sarin causes a rapid (< 1 h) and persistent (up to 7 days) increase of GFAP in different brain areas of rats (Damodaran et al., 2002). Compared to our results, this suggests that NF-κB could be another regulating factor of the astrocytic response to CNS injury induced by NA exposure, where the observed increase of TNF-α 24-h post-NIMP exposure could be the triggering event. This hypothesis could be tested using TNF-α inhibitors, and mice exposed to 0.5 LD_{50} of NIMP. Somehow, the 0.5 LD_{50} dose of NIMP induced more significant changes than the 0.9 LD50 dose, which could reflect differential microglial and astrocytic phenotype activation states at the studied time points (Maupu et al., 2021).

During neuroinflammation, microglia are known to be the major source of TNF-α (Olmos and Llado, 2014), consistent with our results showing an increase of IBA-1 labelling 24-h post-NIMP exposure. Although, after exposure to sub-lethal doses of NIMP, mice showed limited neuroinflammation with moderate changes in pro-inflammatory cytokines (IL-1β, IL-6, VEGF, MIP-1α and TNF-α), which normalized 1 week after intoxication. Only the mice exposed to 0.9 LD_{50} exhibited a significant persistence of IBA-1 labelling 1-month after NIMP challenge. This is consistent with previous studies showing a transient neuroinflammation after a high dose NA challenge (Collombet, 2011). The remaining neuroinflammation observed at 1-month was suspected to be linked to the delayed neurodegeneration (Collombet, 2011), however in our study no histopathological damage was apparent in NIMP-exposed mice, even after long-term observation. Further studies will be needed to understand the mechanism

supporting the microglial activation persistence, which could elicit long-term deleterious effects, as it impacts neurogenesis, synaptic pruning (Sierra et al., 2014), and promotes neurodegeneration (Maqbool et al., 2013).

Hippocampal cholinergic innervation plays an important role in cognitive and memory processes, specifically in NORT in which hippocampal ACh efflux, α7 nicotinic cholinergic receptors (nAChRs), and muscarinic cholinergic receptors play crucial roles (Jacklin et al., 2015; Li et al., 2013; Stanley et al., 2012). Considering that 1-month post-NIMP exposure the cholinesterase activity in the hippocampus is still not completely restored, alterations in the cholinergic pathway could explain the performance decrement of both groups of NIMP-exposed mice. Also, it could be interesting to investigate if α7 nAChRs are not downregulated, as they are expressed in microglia and are anti-inflammatory (Rahman and Alzarea, 2019). Poor performance in NORT after chronic DFP in rats has already been reported (Terry et al., 2011), but our results emphasize that a single exposure to a sub-lethal dose of NIMP, which could be almost asymptomatic, is enough to disrupt short-term memory. Furthermore, low theta and high theta brainwave distributions are still disrupted 1-month after NIMP exposure in both groups; while in rats, theta oscillations exert a crucial role in coordination with gamma oscillations for the encoding and retrieval of memories during NORT (Trimper et al., 2014). Again, our results highlight that in addition to delta rhythm, low and high theta oscillations could be used as biomarkers of sub-lethal NA intoxication and their long-term disruption could be predictive of cognitive complications.

In conclusion, exposure to sub-lethal NA doses represent a high probability of occurrence in the event of a terrorist attack or a military conflict. Our results have emphasized that brainwave distribution is disrupted quickly after NIMP exposure,

persists for a long time, and could be used as biomarker of intoxication severity and a helpful tool for the prognosis of possible brain damage. Monitoring electrical brain activity should be implemented in the follow-up of exposed victims, even if they did not show obvious signs of intoxication. Historically, sarin has been the most used chemical weapon and still represents a threat. Here, we confirmed NIMP as a potential surrogate of sarin intoxication in mice and as helpful tool to investigate long-term NA effects.

Acknowledgments

This work used the imagery and biological analysis platforms of IRBA supported by the Service de Santé des Armées. We particularly thank Xavier Butigieg and Cédric Castellerin for technical support.

Funding sources

This work was supported by the French Ministry of Armed Forces: Direction Générale de l'Armement (DGA) and Service de Santé des Armées (SSA). Funding sources had no involvement in study design, collection, analysis or interpretation of data, or decision to publish.

References

Abou-Donia, M.B., Siracuse, B., Gupta, N., and Sobel Sokol, A. (2016). Sarin (GB, O-isopropyl methylphosphonofluoridate) neurotoxicity: critical review. Crit Rev Toxicol *46*, 845-875.

Amend, N., Niessen, K.V., Seeger, T., Wille, T., Worek, F., and Thiermann, H. (2020). Diagnostics and treatment of nerve agent poisoning-current status and future developments. Ann N Y Acad Sci *1479*, 13-28.

Amilhon, B., Ducharme, G., Jackson, J., Goutagny, R., and Williams, S. (2020). Theta Rhythm in Hippocampus and Cognition.

Baille, V., Dorandeu, F., Carpentier, P., Bizot, J.C., Filliat, P., Four, E., Denis, J., and Lallement, G. (2001). Acute exposure to a low or mild dose of soman: biochemical, behavioral and histopathological effects. Pharmacol Biochem Behav *69*, 561-569.

Barrientos, R.M., Kitt, M.M., Watkins, L.R., and Maier, S.F. (2015). Neuroinflammation in the normal aging hippocampus. Neuroscience *309*, 84-99.

Bloch-Shilderman, E., Rabinovitz, I., Egoz, I., Yacov, G., Allon, N., and Nili, U. (2018). Determining a threshold sub-acute dose leading to minimal physiological alterations following prolonged exposure to the nerve agent VX in rats. Arch Toxicol *92*, 873-892.

Bokil, H., Andrews, P., Kulkarni, J.E., Mehta, S., and Mitra, P.P. (2010). Chronux: a platform for analyzing neural signals. Journal of neuroscience methods *192*, 146-151.

Buzsáki, G., and Draguhn, A. (2004). Neuronal oscillations in cortical networks. Science (New York, NY) *304*, 1926-1929.

Buzsaki, G., Logothetis, N., and Singer, W. (2013). Scaling brain size, keeping timing: evolutionary preservation of brain rhythms. Neuron *80*, 751-764.

Carpentier, P., Foquin, A., Dorandeu, F., and Lallement, G. (2001). Delta activity as an early indicator for soman-induced brain damage: a review. Neurotoxicology *22*, 299-315.

Chai, P.R., Hayes, B.D., Erickson, T.B., and Boyer, E.W. (2018). Novichok agents: a historical, current, and toxicological perspective. Toxicol Commun *2*, 45-48.

Chambers, J.E., Chambers, H.W., Meek, E.C., and Pringle, R.B. (2013). Testing of novel brain-penetrating oxime reactivators of acetylcholinesterase inhibited by nerve agent surrogates. Chem Biol Interact *203*, 135-138.

Chambers, J.E., and Meek, E.C. (2020). Novel centrally active oxime reactivators of acetylcholinesterase inhibited by surrogates of sarin and VX. Neurobiol Dis *133*, 104487.

Chambers, J.E., Meek, E.C., and Chambers, H.W. (2016). Novel brain-penetrating oximes for reactivation of cholinesterase inhibited by sarin and VX surrogates. Ann N Y Acad Sci *1374*, 52-58.

Collombet, J.M. (2011). Nerve agent intoxication: recent neuropathophysiological findings and subsequent impact on medical management prospects. Toxicol Appl Pharmacol *255*, 229-241.

Crouzier, D., Le Crom, V.B., Four, E., Lallement, G., and Testylier, G. (2004). Disruption of mice sleep stages induced by low doses of organophosphorus compound soman. Toxicology *199*, 59-71.

Dail, M.B., Leach, C.A., Meek, E.C., Olivier, A.K., Pringle, R.B., Green, C.E., and Chambers, J.E. (2019). Novel Brain-Penetrating Oxime Acetylcholinesterase Reactivators Attenuate Organophosphate-Induced Neuropathology in the Rat Hippocampus. Toxicol Sci *169*, 465-474.

Damodaran, T.V., Bilska, M.A., Rahman, A.A., and Abou-Doni, M.B. (2002). Sarin causes early differential alteration and persistent overexpression in mRNAs coding for glial fibrillary acidic protein (GFAP) and vimentin genes in the central nervous system of rats. Neurochem Res *27*, 407-415.

Damodaran, T.V., Rahman, A.A., and Abou-Donia, M.B. (2000). Early differential induction of C-jun in the central nervous system of hens treated with diisopropylphosphorofluoridate (DFP). Neurochem Res *25*, 1579-1586.

de Araujo Furtado, M., Lumley, L.A., Robison, C., Tong, L.C., Lichtenstein, S., and Yourick, D.L. (2010). Spontaneous recurrent seizures after status epilepticus induced by soman in Sprague-Dawley rats. Epilepsia *51*, 1503-1510.
Duffy, F.H., Burchfiel, J.L., Bartels, P.H., Gaon, M., and Sim, V.M. (1979). Long-term effects of an organophosphate upon the human electroencephalogram. Toxicol Appl Pharmacol *47*, 161-176.
Eddleston, M. (2019). Novel Clinical Toxicology and Pharmacology of Organophosphorus Insecticide Self-Poisoning. Annu Rev Pharmacol Toxicol *59*, 341-360.
Enderlin, J., Igert, A., Auvin, S., Nachon, F., Dal Bo, G., and Dupuis, N. (2020). Characterization of organophosphate-induced brain injuries in a convulsive mouse model of diisopropylfluorophosphate exposure. Epilepsia *61*, e54-e59.
Fernández-Bouzas, A., Harmony, T., Bosch, J., Aubert, E., Fernández, T., Valdés, P., Silva, J., Marosi, E., Martínez-López, M., and Casián, G. (1999). Sources of abnormal EEG activity in the presence of brain lesions. Clinical EEG (electroencephalography) *30*, 46-52.
Fernández-Bouzas, A., Harmony, T., Fernández, T., Ricardo-Garcell, J., Casián, G., and Sánchez-Conde, R. (2001). Cerebral blood flow and sources of abnormal EEG activity (VARETA) in neurocysticercosis. Clinical neurophysiology : official journal of the International Federation of Clinical Neurophysiology *112*, 2281-2287.
Filliat, P., Baubichon, D., Burckhart, M.F., Pernot-Marino, I., Foquin, A., Masqueliez, C., Perrichon, C., Carpentier, P., and Lallement, G. (1999). Memory impairment after soman intoxication in rat: correlation with central neuropathology. Improvement with anticholinergic and antiglutamatergic therapeutics. Neurotoxicology *20*, 535-549.
França, A.S., do Nascimento, G.C., Lopes-dos-Santos, V., Muratori, L., Ribeiro, S., Lobão-Soares, B., and Tort, A.B. (2014). Beta2 oscillations (23-30 Hz) in the mouse hippocampus during novel object recognition. The European journal of neuroscience *40*, 3693-3703.
Genovese, R.F., Mioduszewski, R.J., Benton, B.J., Pare, M.A., and Cooksey, J.A. (2009). Behavioral evaluation of rats following low-level inhalation exposure to sarin. Pharmacol Biochem Behav *91*, 517-525.
Gf, P., and Franklin, K. (2003). The Mouse Brain In Stereotaxic Coordinates, Vol 1.
González, E.A., Rindy, A.C., Guignet, M.A., Calsbeek, J.J., Bruun, D.A., Dhir, A., Andrew, P., Saito, N., Rowland, D.J., Harvey, D.J*., et al.* (2020). The chemical convulsant diisopropylfluorophosphate (DFP) causes persistent neuropathology in adult male rats independent of seizure activity. Arch Toxicol *94*, 2149-2162.
Grauer, E., Chapman, S., Rabinovitz, I., Raveh, L., Weissman, B.A., Kadar, T., and Allon, N. (2008). Single whole-body exposure to sarin vapor in rats: long-term neuronal and behavioral deficits. Toxicol Appl Pharmacol *227*, 265-274.
Greathouse, B., Zahra, F., and Brady, M.F. (2020). Acetylcholinesterase Inhibitors Toxicity. In StatPearls (Treasure Island (FL): StatPearls Publishing

Guidera, J.A., Taylor, N.E., Lee, J.T., Vlasov, K.Y., Pei, J., Stephen, E.P., Mayo, J.P., Brown, E.N., and Solt, K. (2017). Sevoflurane Induces Coherent Slow-Delta Oscillations in Rats. Frontiers in neural circuits *11*, 36.
Hobson, B.A., Rowland, D.J., Supasai, S., Harvey, D.J., Lein, P.J., and Garbow, J.R. (2018). A magnetic resonance imaging study of early brain injury in a rat model of acute DFP intoxication. Neurotoxicology *66*, 170-178.
Hulet, S.W., McDonough, J.H., and Shih, T.M. (2002). The dose-response effects of repeated subacute sarin exposure on guinea pigs. Pharmacol Biochem Behav *72*, 835-845.

Jacklin, D.L., Kelly, P., Bianchi, C., MacDonald, T., Traquair, H., and Winters, B.D. (2015). Evidence for a specific role for muscarinic receptors in crossmodal object recognition in rats. Neurobiol Learn Mem *118*, 125-132.
Jayakumar, A.R., Tong, X.Y., Ruiz-Cordero, R., Bregy, A., Bethea, J.R., Bramlett, H.M., and Norenberg, M.D. (2014). Activation of NF-kappaB mediates astrocyte swelling and brain edema in traumatic brain injury. J Neurotrauma *31*, 1249-1257.
Jin, G., Bai, D., Yin, S., Yang, Z., Zou, D., Zhang, Z., Li, X., Sun, Y., and Zhu, Q. (2016). Silibinin rescues learning and memory deficits by attenuating microglia activation and preventing neuroinflammatory reactions in SAMP8 mice. Neurosci Lett *629*, 256-261.
John, H., van der Schans, M.J., Koller, M., Spruit, H.E.T., Worek, F., Thiermann, H., and Noort, D. (2017). Fatal sarin poisoning in Syria 2013: forensic verification within an international laboratory network. Forensic Toxicology *36*, 61-71.
Karunakaran, S., Grasse, D.W., and Moxon, K.A. (2016). Role of CA3 theta-modulated interneurons during the transition to spontaneous seizures. Exp Neurol *283*, 341-352.
Kassa, J., Krejcova, G., Skopec, F., Herink, J., Bajgar, J., Sevelova, L., Tichy, M., and Pecka, M. (2004). The influence of sarin on various physiological functions in rats following single or repeated low-level inhalation exposure. Inhal Toxicol *16*, 517-530.
Lee, K., Bohnert, S., Bouchard, M., Vair, C., Farrell, J.S., Teskey, G.C., Mikler, J., and Dunn, J.F. (2020). Quantitative T2 MRI is predictive of neurodegeneration following organophosphate exposure in a rat model. Sci Rep *10*, 13007.
Li, S., Nai, Q., Lipina, T.V., Roder, J.C., and Liu, F. (2013). α7nAchR/NMDAR coupling affects NMDAR function and object recognition. Molecular brain *6*, 58.
Löscher, W., and Friedman, A. (2020). Structural, Molecular, and Functional Alterations of the Blood-Brain Barrier during Epileptogenesis and Epilepsy: A Cause, Consequence, or Both? International journal of molecular sciences *21*.
Lumley, L.A., Rossetti, F., de Araujo Furtado, M., Marrero-Rosado, B., Schultz, C.R., Schultz, M.K., Niquet, J., and Wasterlain, C.G. (2019). Dataset of EEG power integral, spontaneous recurrent seizure and behavioral responses following combination drug therapy in soman-exposed rats. Data in brief *27*, 104629.
Ma, X., Zhang, Y., Wang, L., Li, N., Barkai, E., Zhang, X., Lin, L., and Xu, J. (2020). The Firing of Theta State-Related Septal Cholinergic Neurons Disrupt Hippocampal Ripple Oscillations via Muscarinic Receptors. J Neurosci *40*, 3591-3603.
Maqbool, A., Lattke, M., Wirth, T., and Baumann, B. (2013). Sustained, neuron-specific IKK/NF-κB activation generates a selective neuroinflammatory response promoting local neurodegeneration with aging. Molecular neurodegeneration *8*, 40.
Marciniak, E., Faivre, E., Dutar, P., Alves Pires, C., Demeyer, D., Caillierez, R., Laloux, C., Buée, L., Blum, D., and Humez, S. (2015). The Chemokine MIP-1α/CCL3 impairs mouse hippocampal synaptic transmission, plasticity and memory. Sci Rep *5*, 15862.
Markand, O.N. (1984). Electroencephalography in diffuse encephalopathies. Journal of clinical neurophysiology : official publication of the American Electroencephalographic Society *1*, 357-407.
Marrero-Rosado, B.M., de Araujo Furtado, M., Kundrick, E.R., Walker, K.A., Stone, M.F., Schultz, C.R., Nguyen, D.A., and Lumley, L.A. (2020). Ketamine as adjunct to midazolam treatment following soman-induced status epilepticus reduces seizure severity, epileptogenesis, and brain pathology in plasma carboxylesterase knockout mice. Epilepsy & behavior : E&B *111*, 107229.
Maupu, C., Enderlin, J., Igert, A., Oger, M., Auvin, S., Hassan-Abdi, R., Soussi-Yanicostas, N., Brazzolotto, X., Nachon, F., Dal Bo, G.*, et al.* (2021). Diisopropylfluorophosphate-induced status epilepticus drives complex glial cell phenotypes in adult male mice. Neurobiol Dis *152*, 105276.

Meek, E.C., Chambers, H.W., Coban, A., Funck, K.E., Pringle, R.B., Ross, M.K., and Chambers, J.E. (2012). Synthesis and in vitro and in vivo inhibition potencies of highly relevant nerve agent surrogates. Toxicol Sci *126*, 525-533.
Meffert, M.K., Chang, J.M., Wiltgen, B.J., Fanselow, M.S., and Baltimore, D. (2003). NF-kappa B functions in synaptic signaling and behavior. Nature neuroscience *6*, 1072-1078.
Moncunill, G., Campo, J.J., and Dobaño, C. (2014). Quantification of multiple cytokines and chemokines using cytometric bead arrays. Methods in molecular biology (Clifton, NJ) *1172*, 65-86.
Niijima, H., Nagao, M., Nakajima, M., Takatori, T., Iwasa, M., Maeno, Y., Koyama, H., and Isobe, I. (2000). The effects of sarin-like and soman-like organophosphorus agents on MAPK and JNK in rat brains. Forensic science international *112*, 171-178.
Ohta, H., Ohmori, T., Suzuki, S., Ikegaya, H., Sakurada, K., and Takatori, T. (2006). New safe method for preparation of sarin-exposed human erythrocytes acetylcholinesterase using non-toxic and stable sarin analogue isopropyl p-nitrophenyl methylphosphonate and its application to evaluation of nerve agent antidotes. Pharm Res *23*, 2827-2833.
Olmos, G., and Llado, J. (2014). Tumor necrosis factor alpha: a link between neuroinflammation and excitotoxicity. Mediators Inflamm *2014*, 861231.
Oswal, D.P., Garrett, T.L., Morris, M., and Lucot, J.B. (2013). Low-dose sarin exposure produces long term changes in brain neurochemistry of mice. Neurochem Res *38*, 108-116.
Pearce, P.C., Crofts, H.S., Muggleton, N.G., Ridout, D., and Scott, E.A. (1999). The effects of acutely administered low dose sarin on cognitive behaviour and the electroencephalogram in the common marmoset. Journal of psychopharmacology (Oxford, England) *13*, 128-135.
Phelan, K.D., Shwe, U.T., Williams, D.K., Greenfield, L.J., and Zheng, F. (2015). Pilocarpine-induced status epilepticus in mice: A comparison of spectral analysis of electroencephalogram and behavioral grading using the Racine scale. Epilepsy Res *117*, 90-96.
Pringle, R.B., Meek, E.C., Chambers, H.W., and Chambers, J.E. (2018). Neuroprotection From Organophosphate-Induced Damage by Novel Phenoxyalkyl Pyridinium Oximes in Rat Brain. Toxicol Sci *166*, 420-427.
Rahman, S., and Alzarea, S. (2019). Glial mechanisms underlying major depressive disorder: Potential therapeutic opportunities. Prog Mol Biol Transl Sci *167*, 159-178.
Schultz, M.K., Wright, L.K., de Araujo Furtado, M., Stone, M.F., Moffett, M.C., Kelley, N.R., Bourne, A.R., Lumeh, W.Z., Schultz, C.R., Schwartz, J.E*., et al.* (2014). Caramiphen edisylate as adjunct to standard therapy attenuates soman-induced seizures and cognitive deficits in rats. Neurotoxicol Teratol *44*, 89-104.
Scremin, O.U., Shih, T.M., Huynh, L., Roch, M., Booth, R., and Jenden, D.J. (2003). Delayed neurologic and behavioral effects of subtoxic doses of cholinesterase inhibitors. The Journal of pharmacology and experimental therapeutics *304*, 1111-1119.
Senanayake, N., de Silva, H.J., and Karalliedde, L. (1993). A scale to assess severity in organophosphorus intoxication: POP scale. Hum Exp Toxicol *12*, 297-299.
Shi, M., Deng, S., Cui, Y., Chen, X., Shi, T., Song, L., Zhang, R., Zhang, Y., Xu, J., Shi, J*., et al.* (2021). Repeated low-dose exposures to sarin disrupted the homeostasis of phospholipid and sphingolipid metabolism in guinea pig hippocampus. Toxicology letters *338*, 32-39.
Shih, T.M., and Romano, J.A. (1988). The effects of choline on soman-induced analgesia and toxicity. Neurotoxicol Teratol *10*, 287-294.
Sierra, A., Beccari, S., Diaz-Aparicio, I., Encinas, J.M., Comeau, S., and Tremblay, M. (2014). Surveillance, phagocytosis, and inflammation: how never-resting microglia influence adult hippocampal neurogenesis. Neural plasticity *2014*, 610343.
Stanley, E.M., Wilson, M.A., and Fadel, J.R. (2012). Hippocampal neurotransmitter efflux during one-trial novel object recognition in rats. Neurosci Lett *511*, 38-42.

Terry, A.V., Jr., Buccafusco, J.J., Gearhart, D.A., Beck, W.D., Middlemore-Risher, M.L., Truan, J.N., Schwarz, G.M., Xu, M., Bartlett, M.G., Kutiyanawala, A.*, et al.* (2011). Repeated, intermittent exposures to diisopropylfluorophosphate in rats: protracted effects on cholinergic markers, nerve growth factor-related proteins, and cognitive function. Neuroscience *176*, 237-253.
Testylier, G., Lahrech, H., Montigon, O., Foquin, A., Delacour, C., Bernabe, D., Segebarth, C., Dorandeu, F., and Carpentier, P. (2007). Cerebral edema induced in mice by a convulsive dose of soman. Evaluation through diffusion-weighted magnetic resonance imaging and histology. Toxicol Appl Pharmacol *220*, 125-137.
Timofeeva, O.A., and Gordon, C.J. (2002). EEG spectra, behavioral states and motor activity in rats exposed to acetylcholinesterase inhibitor chlorpyrifos. Pharmacol Biochem Behav *72*, 669-679.
Tonduli, L.S., Testylier, G., Masqueliez, C., Lallement, G., and Monmaur, P. (2001). Effects of Huperzine used as pre-treatment against soman-induced seizures. Neurotoxicology *22*, 29-37.
Trimper, J.B., Stefanescu, R.A., and Manns, J.R. (2014). Recognition memory and theta-gamma interactions in the hippocampus. Hippocampus *24*, 341-353.
van Helden, H.P., Vanwersch, R.A., Kuijpers, W.C., Trap, H.C., Philippens, I.H., and Benschop, H.P. (2004). Low levels of sarin affect the EEG in marmoset monkeys: a pilot study. J Appl Toxicol *24*, 475-483.
Yanagisawa, N., Morita, H., and Nakajima, T. (2006). Sarin experiences in Japan: acute toxicity and long-term effects. J Neurol Sci *249*, 76-85.

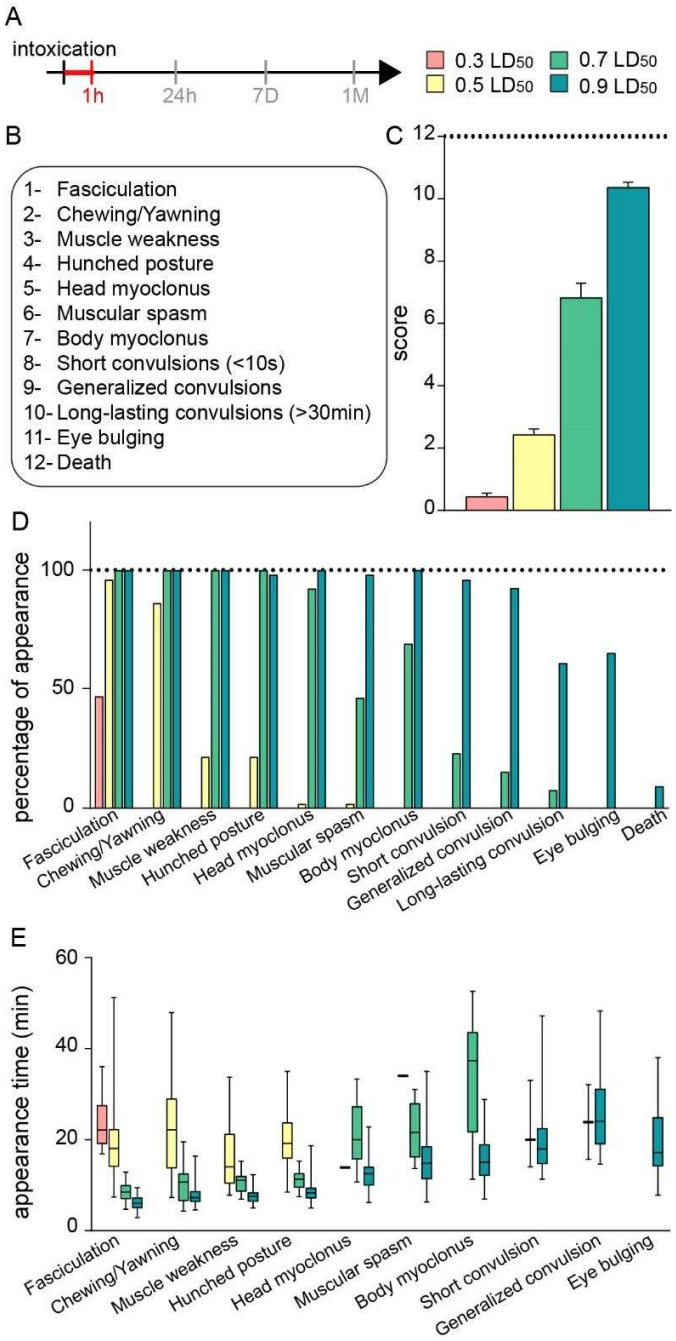

Figure 1: Intoxication severity evaluation. (A) Representation of the experimental design with the time of interest highlighted. (B) Intoxication scale based on the 12 more relevant behavioural changes. (C) Average score induced by the different doses: 0.56 ± 0.13 for 0.3 LD_{50}; 2.45 ± 0.16 for 0.5 LD_{50}; 6.85 ± 0.45 for 0.7 LD_{50} and 10.39 ± 0.15 for

0.9 LD_{50}. Representations of the occurrence percentage (D) and the onset time (E) of each sign that occurs following NIMP exposure.

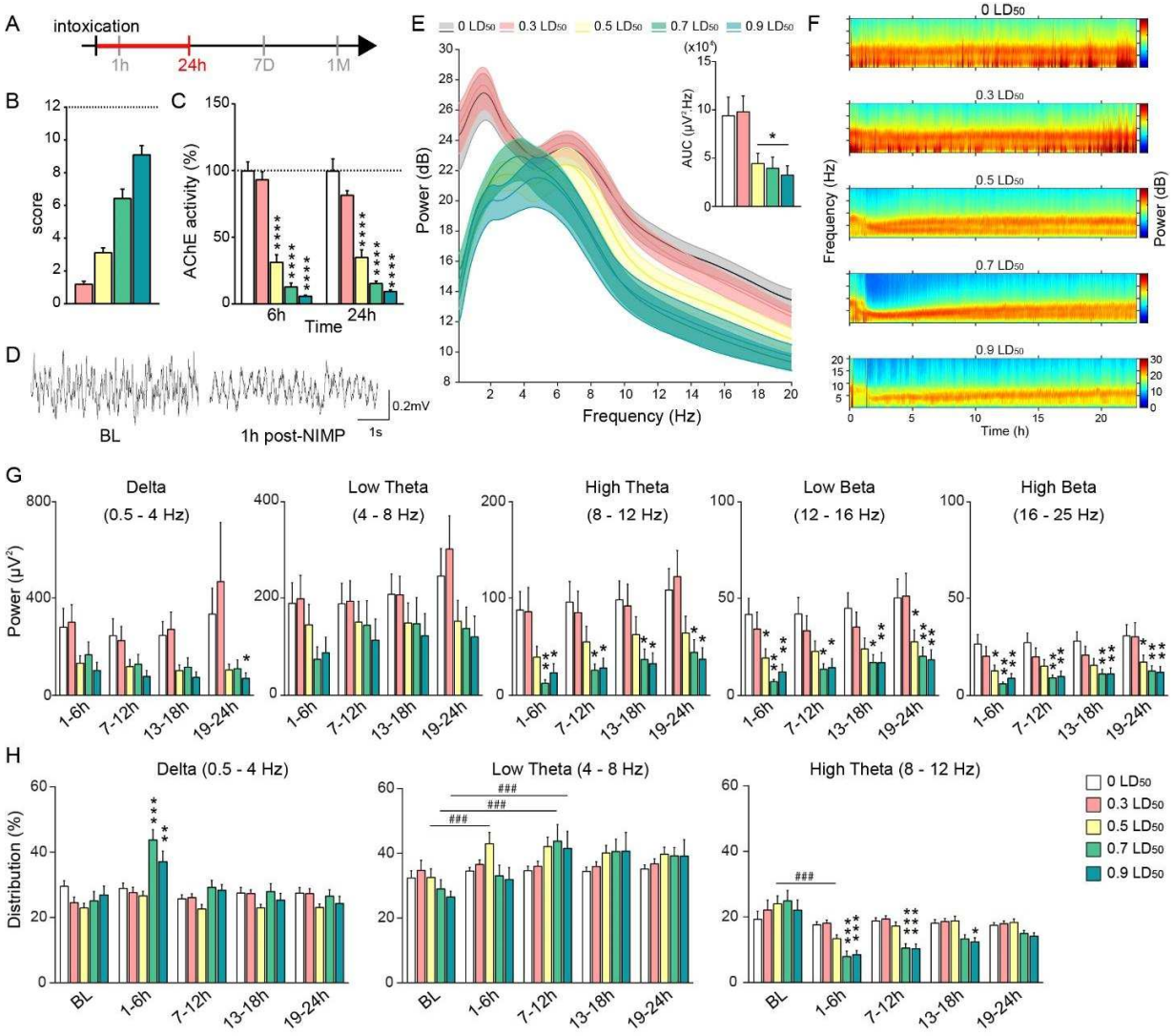

Figure 2: Short term cortical activity modifications. (A) Representation of the experimental design with the time of interest highlighted. (B) Surgery did not modify the average intoxication score obtained after NIMP exposure: 1.21 ± 0.15 for 0.3 LD_{50} (n=14); 3.14 ± 0.27 for 0.5 LD_{50} (n=14); 6.45 ± 0.54 for 0.7 LD_{50} (n=11) and 9.11 ± 0.54 for 0.9 LD_{50} (n=18) (Kruskal-Wallis tests followed by Dunn's post-tests to compare each dose with surgery and without surgery). (C) Inhibition of AChE activity at 6h (100 ± 6.4 for 0 LD_{50}; 93.44 ± 5.7 for 0.3 LD_{50}; 31.7 ± 5.3 for 0.5 LD_{50}; 13.2 ± 2.5 for 0.7 LD_{50} and 6.1 ± 0.5 for 0.9 LD_{50}) and 24h (100 ± 8.7 for 0 LD_{50}; 81.7 ± 3.0 for 0.3 LD_{50}; 35.3 ± 5.3

for 0.5 LD_{50}; 15.7 ± 1.5 for 0.7 LD_{50} and 9.7 ± 1.0 for 0.9 LD_{50}) after NIMP exposure (n=8 per group). Significant differences were determined by one-way ANOVA ($F = 59.54$ $p<0.0001$ for 6h and $F = 41.49$ $p<0.0001$ for 24h) with Dunnett's post hoc tests to compare to CTL group ($p<0.0001$). (D) Examples of non-filtered ECoG signal during the baseline (left) and 1h post- 0.9LD_{50} NIMP exposure recording. (E) Power spectrum representations for each tested dose of NIMP over the 24 hours period. In insert, the area under the curve (AUC) is represented (9.4 $x10^4$ ± 1.9 $x10^4$ for 0 LD_{50} (n=13); 9.8 $x10^4$ ± 1.6 $x10^4$ for 0.3 LD_{50} (n=14); 4.5 $x10^4$ ± 1.0 $x10^4$ for 0.5 LD_{50} (n=14); 4.0 $x10^4$ ± 1.1 $x10^4$ for 0.7 LD_{50} (n=11) and 3.3 $x10^4$ ± 0.9 $x10^4$ for 0.9 LD_{50} (n=18)). Significant differences were determined by one-way ANOVA ($F = 5.0$ $p=0.0017$) with Dunnett's post hoc tests to compare to CTL group (0 LD_{50} vs. 0.5 LD_{50} $p=0.04$; 0 LD_{50} vs. 0.7 LD_{50} $p=0.03$; 0 LD_{50} vs. 0.9 LD_{50} $p=0.01$). (F) Periodograms representation for each tested dose of NIMP over the 24 hours period. (G) Diagrams of each brainwave relative power changes at different time periods that follow NIMP exposure, during the 24 hours of recording. Significant differences were determined by two-way ANOVA repeated measure (Delta: $F_{dose} = 4.6$ $p=0.003$; Low theta: $F_{dose} = 1.5$ $p=0.2$; High theta: $F_{dose} = 22.2$ $p=0.003$; Low beta: $F_{dose} = 23.9$ $p=0.001$; High beta: $F_{dose} = 24.3$ $p=0.01$) with Dunnett's post hoc tests to compare to CTL group. (H) Diagrams of each brainwave distribution changes at different time periods that follow NIMP exposure, during the 24 hours of recording. Significant differences were determined by two-way ANOVA repeated measure (Delta: $F_{time} = 22.1$ $p<0.0001$, $F_{dose} = 4.6$ $p=0.003$; Low theta: $F_{time} = 18.5$ $p<0.0001$, $F_{dose} = 0.7$ $p=0.6$; High theta: $F_{time} = 33.7$ $p<0.0001$, $F_{dose} = 8.5$ $p<0.0001$) with Dunnett's post hoc tests to compare to CTL group or to baseline.

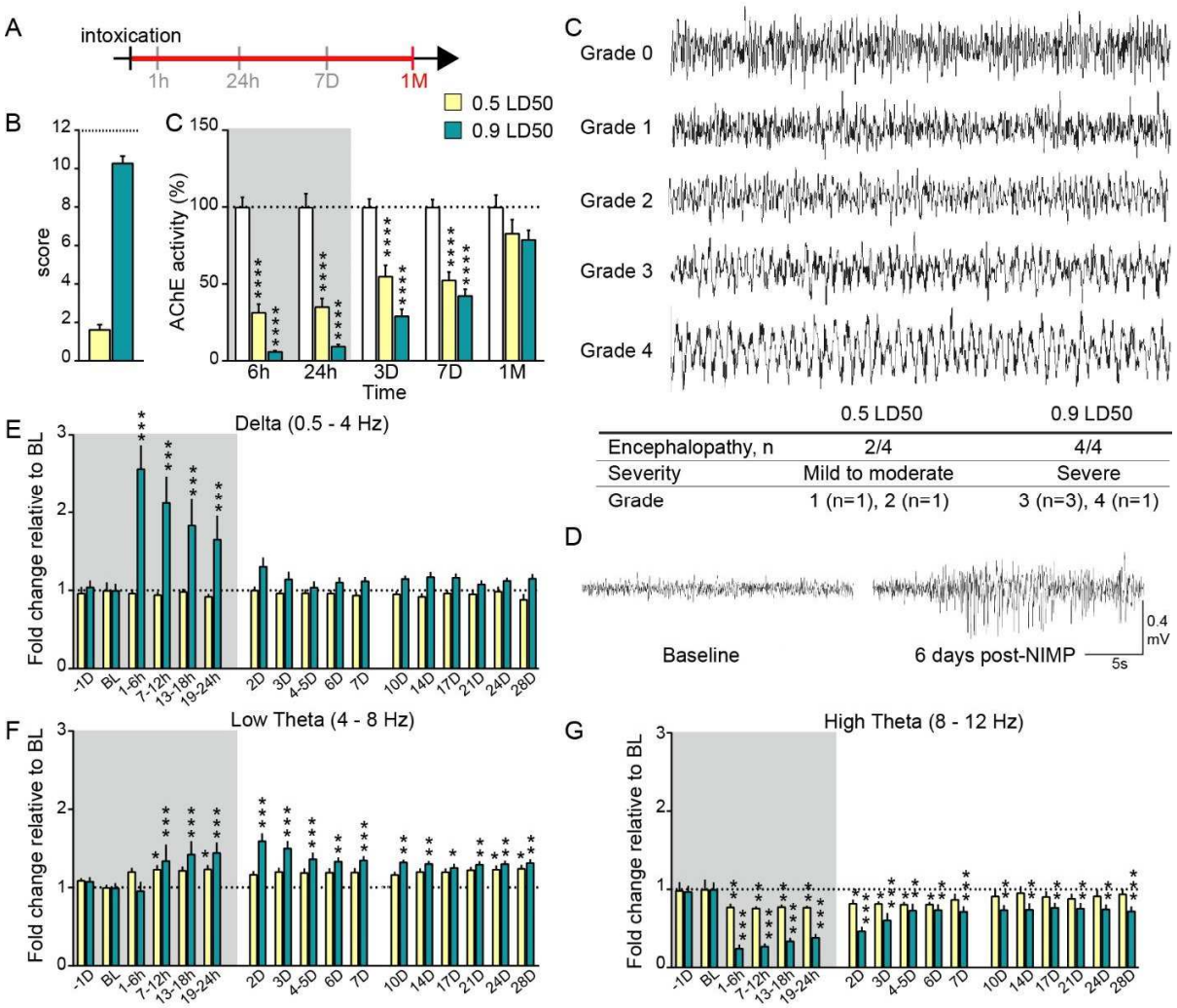

Figure 3: Cortical activity modifications at longer term. (A) Representation of the experimental design with the time of interest highlighted. (B) Surgery did not change the average intoxication score obtained after NIMP exposure: 1.6 ± 0.2 for 0.5 LD_{50} (n=11); and 10.3 ± 0.4 for 0.9 LD_{50} (n=11) (Kruskal-Wallis tests followed by Dunn's post-tests to compare each dose with surgery and without surgery). (C) Inhibition of AChE activity was evaluated at several time points after NIMP exposure: 3 days (100 ± 5.3 for 0 LD_{50}; 55.1 ± 7.1 for 0.5 LD_{50} and 29.3 ± 4.2 for 0.9 LD_{50}); 7 days (100 ± 5.0 for 0 LD_{50}; 52.6 ± 5.2 for 0.5 LD_{50} and 42.5 ± 4.1 for 0.9 LD_{50}) and 1-month (100 ± 7.9 for 0 LD_{50}; 83.1 ± 8.8 for 0.5 LD_{50} and 79.0 ± 5.9 for 0.9 LD_{50}) (n=8 per group). Significant differences

were determined by one-way ANOVA ($F = 44.9$ $p<0.0001$ for 3D; $F = 44$ $p<0.0001$ for 7D and $F = 2.2$ $p=0.15$ for 1M) with Dunnett's post hoc tests to compare to CTL group ($p<0.0001$). (C) ECoG stratification for grading mice encephalopathy according to Markand's: Grade 0 (Normal ECoG): Quiet wakefulness stage at 7 Hz and amplitude of 150/200 µv ; Grade 1: Wakefulness stage with 5-7 Hz background activity; Grade 2: Wakefulness stage at 4-6 Hz background activity and amplitude of 100/200 µV; Grade 3: Wakefulness stage at 3 Hz background activity and amplitude of 150/200 µV; Grade 4: Wakefulness stage with monomorphic and monotonous delta 2.5 Hz background activity and amplitude of 200 µV. The table highlights the number of evaluated animals, the severity and the grade reached depending of the dose of NIMP. (D) Examples of non-filtered ECoG recording during the baseline (left) and 6 days post- 0.5 LD_{50} NIMP exposure showing a "spike and wave"-like discharge. (E-G) Diagrams of the changes in brainwave distribution at different time periods following NIMP exposure over 1-month. Significant differences were determined by two-way ANOVA repeated measure Significant differences were determined by two-way ANOVA repeated measure (Delta: $F_{time} = 10.9$ $p<0.0001$, $F_{dose} = 13.8$ $p=0.002$; Low theta: $F_{time} = 16.9$ $p<0.0001$, $F_{dose} = 5.7$ $p=0.04$; High theta: $F_{time} = 28.9$ $p<0.0001$, $F_{dose} = 14.5$ $p=0.008$) with Dunnett's post hoc tests to compare to baseline.

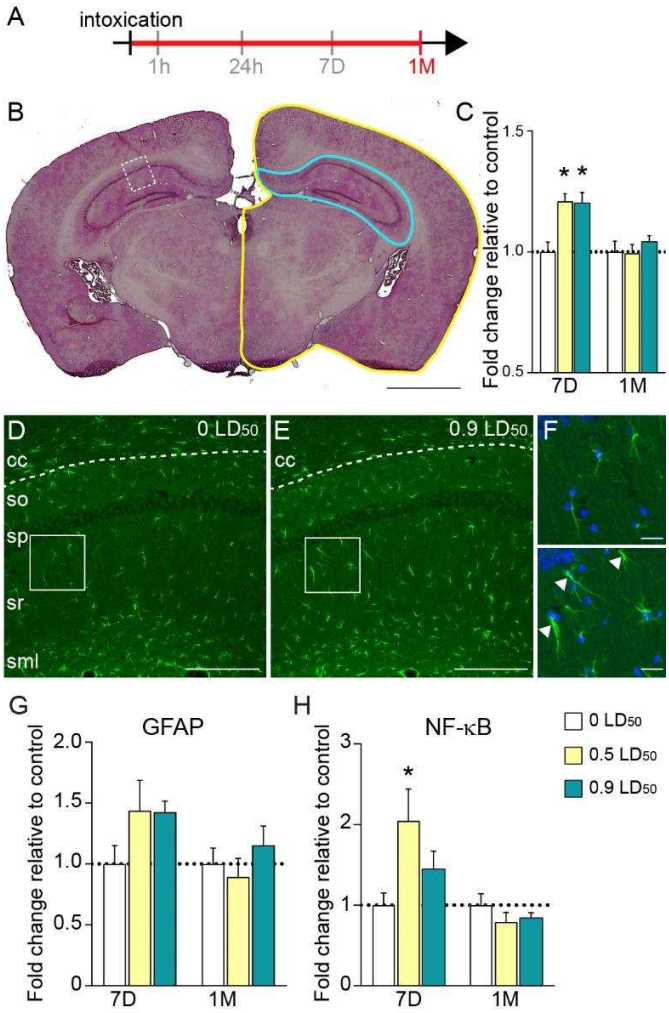

Figure 4: Neuroanatomical modifications induced by exposition to sub-lethal doses of NIMP. (A) Representation of the experimental design with the time of interest highlighted. (B) Image of a coronal brain section after HPS staining showing the selected areas of full hemisphere (yellow surrounding) and HF (blue surrounding). Dot box show CA1 imaged in D. Scale bar = 2mm. (C) Diagram of the ratio of HF over total hemisphere areas normalized to CTL at 7 days post-intoxication: 1.0 ± 0.04 for 0 LD_{50}; 1.21 ± 0.03 for 0.5 LD_{50} and 1.20 ± 0.04 for 0.9 LD_{50} and 1-month post-intoxication: 1.0 ± 0.04 for 0 LD_{50}; 0.99 ± 0.04 for 0.5 LD_{50} and 1.04 ± 0.02 for 0.9 LD_{50} (n=5 per group). Significant differences were determined by Kruskal-Wallis tests (p=0.004 and 0.63 for

7D and 1M respectively) followed by Dunn's po*st*-test to compare to CTL. (D-E) Pictures of GFAP labelling in CA1 of CTL (D) and 0.9 LD_{50} (E) mice. Scale bar = 200µm. (F) Magnification of the white boxes embedded in images D and E, showing the increased reactivity of astrocytes in 0.9 LD_{50} (bottom) hippocampus compared to the CTL's one (top). Scale bar = 20µm. (G) Diagram of GFAP labelling optical density percentage normalized with CTL values at 7 days post-intoxication: 1.0 ± 0.15 for 0 LD_{50}; 1.44 ± 0.25 for 0.5 LD_{50} and 1.43 ± 0.09 for 0.9 LD_{50} and 1-month post-intoxication: 1.0 ± 0.13 for 0 LD_{50}; 0.89 ± 0.15 for 0.5 LD_{50} and 1.15 ± 0.16 for 0.9 LD_{50} (n=5 per group). Statistical differences were determined by Kruskal-Wallis tests (p=0.27 and 0.45 for 7D and 1M respectively). (H) Diagram of NF-κB expression levels normalized to CTL values at 7 days post-intoxication: 1.0 ± 0.15 for 0 LD_{50}; 2.05 ± 0.39 for 0.5 LD_{50} and 1.45 ± 0.22 for 0.9 LD_{50} and 1-month post-intoxication: 1.0 ± 0.14 for 0 LD_{50}; 0.79 ± 0.11 for 0.5 LD_{50} and 0.84 ± 0.07 for 0.9 LD_{50} (n=8 per group). Significant differences were determined by Kruskal-Wallis tests (p=0.04 and 0.61 for 7D and 1M respectively) followed by Dunn's post-test to compare to CTL.

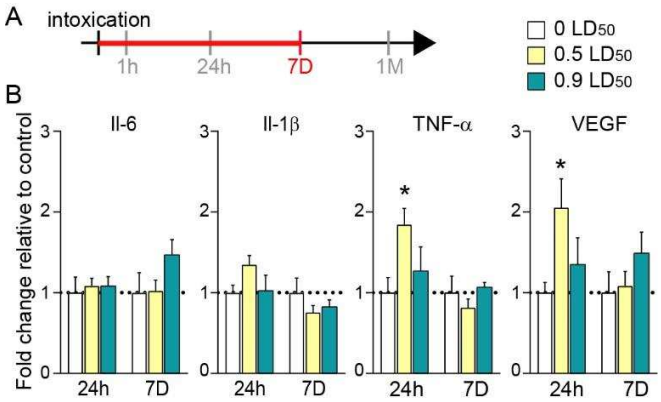

Figure 5: Transient cytokines levels elevation induced by sub-lethal doses of NIMP. (A) Representation of the experimental design with the time of interest highlighted. (B) Diagrams of Il-6, Il-1β, TNF-α and VEGF expression levels normalized with CTL values at 24 hours post-intoxication [(Il-6: 1.0 ± 0.10 for 0 LD_{50}; 1.2 ± 0.05 for 0.5 LD_{50} and 1.13 ± 0.24 for 0.9 LD_{50}); (Il-1β: 1.0 ± 0.09 for 0 LD_{50}; 1.35 ± 0.11 for 0.5 LD_{50} and 1.02 ± 0.19 for 0.9 LD_{50}); (TNF-α: 1.0 ± 0.19 for 0 LD_{50}; 1.85 ± 0.20 for 0.5 LD_{50} and 1.27 ± 0.30 for 0.9 LD_{50}); (VEGF: 1.0 ± 0.13 for 0 LD_{50}; 2.05 ± 0.36 for 0.5 LD_{50} and 1.35 ± 0.33 for 0.9 LD_{50})] and 7 days post-intoxication [(Il-6: 1.0 ± 0.13 for 0 LD_{50}; 0.87 ± 0.10 for 0.5 LD_{50} and 1.06 ± 0.13 for 0.9 LD_{50}); (Il-1β: 1.0 ± 0.18 for 0 LD_{50}; 0.75 ± 0.09 for 0.5 LD_{50} and 0.82 ± 0.08 for 0.9 LD_{50}); (TNF-α:1.0 ± 0.21 for 0 LD_{50}; 0.81 ± 0.11 for 0.5 LD_{50} and 1.07 ± 0.06 for 0.9 LD_{50}); (VEGF: 1.0 ± 0.26 for 0 LD_{50}; 1.08 ± 0.18 for 0.5 LD_{50} and 1.49 ± 0.26 for 0.9 LD_{50})] (n=8 per group). Significant differences were determined by Kruskal-Wallis tests (p=0.03 and 0.04 for TNF-α and VEGF respectively at 24h post-intoxication) followed by Dunn's post-tests to compare to CTL.

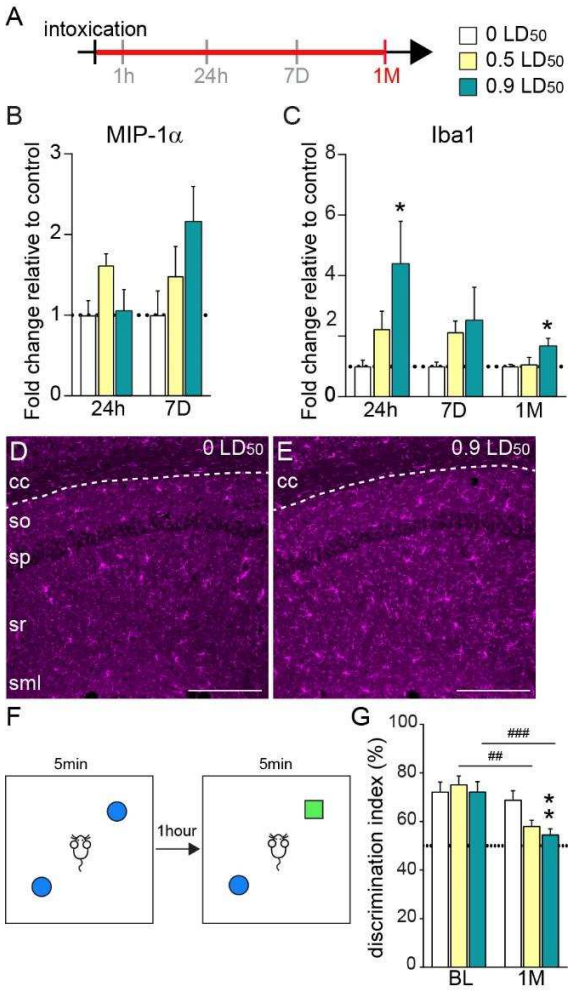

Figure 6: Neuroinflammatory activation and plasticity memory impairment induced by sub-lethal doses of NIMP. (A) Representation of the experimental design with the time of interest highlighted. (B) Diagram of MIP-1α expression levels normalized to CTL at 24 hours: 1.0 ± 0.18 for 0 LD_{50}; 1.62 ± 0.14 for 0.5 LD_{50} and 1.06 ± 0.26 for 0.9 LD_{50} and 7 days post-intoxication: 1.0 ± 0.3 for 0 LD_{50}; 1.48 ± 0.37 for 0.5 LD_{50} and 2.16 ± 0.43 for 0.9 LD_{50} (n=8 per group). Statistical differences were determined by Kruskal-Wallis test (p=0.12 and 0.25 for 24h and 7D respectively). (C) Diagram of IBA1 labelling optical density percentage normalized to CTL at 24 hours post-intoxication: 1.0 ± 0.20 for 0 LD_{50}; 2.24 ± 0.59 for 0.5 LD_{50} and 4.39 ± 1.40 for 0.9 LD_{50}; 7 days post-intoxication:

1.0 ± 0.14 for 0 LD_{50}; 2.13 ± 0.37 for 0.5 LD_{50} and 2.53 ± 1.09 for 0.9 LD_{50}; and 1-month post-intoxication: 1.0 ± 0.07 for 0 LD_{50}; 1.06 ± 0.23 for 0.5 LD_{50} and 1.67 ± 0.25 for 0.9 LD_{50} (n=5 per group). Significant differences were determined by Kruskal-Wallis tests (p=0.03, p=0.15 and 0.03 for 24h, 7D and 1M respectively) followed by Dunn's post-tests to compare to CTL. (D-E) Pictures of IBA-1 labelling in CA1 region of CTL (D) and 0.9 LD_{50} (E) mice. Scale bar = 200µm. (F) Experimental representation of the novel object recognition test. (G) Diagram of the discrimination index corresponding to the percentage of the time for the novel object percentage during the exploration session. Baseline: 72.37 ± 3.88% for 0 LD_{50} (n=15); 73.37 ± 3.46% for 0.5 LD_{50} (n=15) and 72.39 ± 3.95 for 0.9 LD_{50} (n=17); and 1-month post-intoxication: 69.06 ± 3.63% for 0 LD_{50}; 58.23 ± 2.35% for 0.5 LD_{50} and 54.69 ± 2.31 for 0.9 LD_{50}. Significant differences were determined by two-way ANOVA repeated measure (F_{time} = 19.44 $p<0.0001$, F_{dose} = 4.2 p=0.10) with Bonferroni's post hoc tests to compare to baseline (marked with #; p=0.002 and p=0.0004 for 0.5 LD_{50} and 0.9 LD_{50} respectively) or Dunnet's post hoc tests to compare to CTL group (p=0.06 and p=0.007 for 0.5 LD_{50} and 0.9 LD_{50} respectively at 1-month post-intoxication).